

Investigation and Improvement of
Zinc Electrodes for Electrochemical Cells

Quarterly Report No. 1
July to September, 1964
Contract No. NAS 5-3873

National Aeronautics and Space Administration
Goddard Flight Center
Greenbelt, Maryland

Yardney Electric Corporation
New York, New York

Prepared by: 
Z.O.J. Stachurski


Dr. U.A. Dalin


Approved by: Frank Solomon, AVP

TABLE OF CONTENTS

1. Introduction
2. Results and Discussion
 - 2.1 Microscopic Investigation of Morphology and Growth of Zinc Deposits
 - 2.1.1 Study of the Growth Process
 - 2.1.2 Examination of the Zinc Foam
 - 2.1.3 Examination of the Penetrated Cellophane Separators from Microcells
 - 2.2 Zinc Penetration in Regular Ag/Zn Cycled Cell
 - 2.3 Kinetic Study of Zinc Deposition
 - 2.4 Study of Membrane Properties Significant for Penetration
3. Summary and Conclusions
4. Program for Next Quarter

1. INTRODUCTION

The principal objective of this work is to find and explain the phenomena underlying zinc deposition and penetration through separators in alkaline cells. The physico-chemical system involved here is rather complex. We attempt therefore to separate its variables in such a way as will permit us to obtain quantitative data concerning parameters related to each phenomenon. Once we will have such data, an attempt will be made to build a quantitative electrochemical model of zinc penetration. It is understood that such a theoretical model will help us to better the cells containing zinc/semipermeable membrane systems. We are planning to do our work in the following stages: qualitative picture of the formation of deposit and of penetration through cellophane; quantitative picture of penetration; elaboration of quantitative model of penetration mechanism, and its testing; attempt to improve the zinc electrode based on the theory. At every stage of our work, we will pay attention to the morphology of the deposits and electrochemical kinetics of their formation, both for free growth in the solution as well as in the separator. The influence of surface active substances resulting from cellophane decay and other impurities will be studied as part of this work.

Such an influence was investigated by Kriukova (A. d. Nauk. SSSR-Trudy i Soveshtch. Elektrokhim, Moscow 1959, pp 762-767). Her paper is the main literature position pertaining to the zinc penetration problem.

2. RESULTS AND DISCUSSION

2.1 Microscopic Investigation of Morphology and Growth of Zinc Deposits

Electrodeposition of zinc was conducted in cells designed for microscopic investigation of deposits and separators, while the current flows. Such a cell is shown in Figure 1, and its cross section in Figure 2. Electrodes of the cell were made of zinc sheet (0.025"). The cathode (7) was covered by a thin layer of epoxy resin (8) except for the edge in front of the anode (4). Cathodes were tested both with and without separator (0.0010 cellophane, DuPont PUDO-300). In parallel with the cathode was placed a reference zinc electrode (5). Electrodes were connected either to a potentiostat (Wenking) (1) or to a galvanostatic system. The transparent cell case was made of plexiglass with polyethylene washers (3). A microscope cover-glass formed one wall of the cell (9). A metallographic microscope (2) was used for making pictures. Above described cell we will call a micro-cell. Magnification of 100 diameters was used in taking photo micrographs during the growth of deposits. After the experiments were completed in the micro-cell, the cathode was taken out and the penetrated spots in the separators were investigated at 400 x and 1000 x (immersion).

A third way of examining the deposits was used where they were only loosely aggregated. The deposit was scraped from the plate, shaken with water and then acetone, and dried, after which it was immersed in oil for microscopic examination. Anticipating presentation of results, it is convenient to mention here that in this work we found qualitatively different types of deposits which we classify in four groups:

1. Smooth deposits - dense, with no pores visible even at 1000 x.
 2. Foam - (or light sponge) - soft and weak deposit of low density, and of very fine porosity (porosity invisible at 100 x).
 3. Dendrites - hexagonal elongated crystals, with branches visible at 100 x.
 4. Heavy sponge - visibly porous (at 100 x), rather dense and hard.
- All experiments were done at room temperature.

2.1.1 Study of the Growth Process

Growing of zinc deposits was conducted either potentiostatically or galvanostatically. In the potentiostatic method of growth, an overpotential, η , of zinc was maintained constant versus zinc reference electrode and was independent of changes of the surface of the electrode. Zinc overpotentials in actual Ag/Zn cells during charge vary between -10 mV and -100 mV, a typical value being -15 mV. Values around -100 mV may occur on overcharge of cells. This is the reason why we have chosen a similar range of overpotentials for potentiostatic studies under the microscope.

An example of potentiostatic deposition of zinc at $\eta = -100$ mV in 44% KOH saturated with zincate is given in Figure 5 and Figure 6. The cathode was wrapped in this experiment. The picture of figure 5 was taken at 30 minutes after start and of figure 6, 21 hours after start. Figure 5^b is a drawing corresponding to figure 5 and serves for identification of significant features of the structure. The zinc in this example was deposited as a sponge which became heavier with time. The space between the zinc electrode and separators was filled gradually with sponge. Next, this sponge started growing into the separator (Figure 6^b -3).

A similar experiment in which no separator was present yields a typical dendritic deposit with well formed hexagonal crystals 0.05-0.1 mm in diameter (Fig. 7 and 7^b). On an electrode at a specific overpotential we can have simultaneous formation of heavy sponge and dendrites at different places. For example, figure 8 shows simultaneous formation of heavy sponge and typical dendrites at the corner of the electrodes. After sixteen hours more of plating, all of the free space in this corner of the electrode is filled by heavy sponge, as is evident from figure 9. The cause of the differences in structure of the deposit is undoubtedly local variation in current density. It therefore follows that η affects the form of the deposit only as it affects local current density. Moreover, η is not the only controlling factor, the other being the local concentration of the depositing material, in this case zincate.

Figure 35 shows data from a potentiostatic deposition on a wrapped and on an unwrapped electrode. Curve 2 for the unwrapped electrode is associated with dendrite formation. Curve 1 for the wrapped electrode is associated with heavy sponge formation. The significant point is that the overvoltage was the same for both types of deposit.

In Figure 10 through Figure 12 is shown potentiostatic growth of a dendrite toward a hole in the separator. Through this hole, zincate diffuses more rapidly than through the separator. The local higher concentration of zincate causes a higher Zn deposition current and consequently the formation of well shaped dendrites. The rest of the electrode was covered by heavy sponge.

Potentiostatic plating under similar conditions but at 15 mV overpotential never leads to either dendrite formation or heavy sponge, zinc foam being produced instead. Zinc foam filled the empty space between the separator and the zinc electrode. Penetration of cellophane did not occur under such conditions. To complete the picture, potentiostatic runs were performed with a rotating disc electrode of zinc, and smooth plating resulted at all overpotentials up to -55 mV. (Details in section 2.3). When zinc was plated on a rotating disc from dilute zincate solutions (order of 10^{-3} molar) a heavy coat of zinc foam was obtained. Since in dilute zincate solutions the contribution of concentration overpotential to the total overpotential is high, it can be associated with foam formation.

Galvanostatic penetration of zinc through a cellophane membrane is shown in Figure 13 through Figure 18. Deposition was conducted from 30% KOH saturated with zincate. The total current was 1 mA. The deposit was initially dendritic (Figs. 13 and 14) but turned into a heavy sponge in later stages of deposition (Fig. 15 to 17). After the free space between the separator and zinc sheet was filled by the heavy sponge, penetration started. A cone of zinc starts growing into the separator. This cone does not show the characteristic shape of a dendrite and can be placed between the heavy sponge type and the dendritic type. While the zinc is penetrating the separator, only a slight bulging of the separator is visible. We therefore conclude that the zinc deposit grows within the separator, rather, and does not puncture it mechanically.

After penetration is complete, deposition continues preferentially at the penetrated spot. Visual examination in addition to the photographs indicate that the external deposit is initially dendritic and then changes to spongy and foamy (Figures 16 to 18).

Galvanostatic plating was done also in a cell in which all conditions were the same as above, but the cathode was unwrapped. In this case zinc foam was deposited (Fig. 19 and 20), from the early stage to the moment of short.

2.1.2 Examination of the Zinc Foam

Zinc foam was always obtained in KOH (30-44%) saturated with zincates at low overpotentials, e.g. 15 mV or low geometric current density, e.g. 2 mA/cm². At 100 x it has a cloudy look and seems to be formed of grains (Fig. 21, 22, 23a, 24, 25). When such a grain is further investigated at 1000 x (Fig. 26) it appears that it is formed of very fine whiskers. Diameters of the whiskers are of the order of 0.2 micron to 1 micron. This means that whiskers in sponge are 100 to 1000 x thinner than a typical dendrite. This big difference occurs where the current density is changed by a factor of about 10. This suggests that there must be a qualitative difference in mechanism of dendrite and foam formation. The difference

between the mechanism of dendrite formation and heavy sponge formation seems to be less pronounced. To get further information about zinc foam it was disintegrated to small fractions by shaking with water. The material was then washed in acetone, dried, immersed in immersion oil and inspected microscopically at 1000 x magnification. An example of foam at this magnification is given in Fig. 26 and 23b. The conditions under which the photographs were taken were unsuitable for showing the structure of the whiskers. At the present time, the intention is to examine these by electron microscope, so no attempt was made to show them by optical micrography. Fragments of whiskers were mainly straight or zig-zag. Only a small portion of the fragments was branched. This suggests the structure of foam as consisting of a network of very thin and elongated whiskers, apparently helical, interlaced rather than interconnected with each other. The thickness of the foam's whiskers depends only slightly on the current density within the range of their formation. This is the opposite behavior from that of dendrites.

2.1.3 Examination of Penetrated Cellophane Separators from Micro-Cells

Cellophane separators, penetrated as described above, were removed from the micro-cells and examined microscopically. An example of a separator, penetrated rapidly at constant high overpotential in 4% KOH + zincate is shown in figure 27a. Figures 27b,c,d, show various portions of the same separator at higher magnification. It is evident that at $\eta = 200$ mV a typically dendritic penetration results. Crystalline dendrites are growing in the separator in all directions. There is no preference for growth directly toward the anode. The orientation of every picture is indicated by the arrows. Penetration at the lower potential, $\eta = 100$ mV in the same solution as above leads to the heavy sponge type of penetration (Figure 28). Galvanostatic penetration at the high current density of $15/\text{mA}/\text{cm}^2$ leads again to the pure dendritic type of penetration (Figure 29 and 30).

To make sure that sponge or dendrites were growing within the separator and not upon it, the zinc was dissolved in dilute H_2SO_4 . Tunnels were visible in the separator reflecting the structure of dendrites. Inspection of cellophane separators from micro-cells in which penetration occurred at medium current ($J = 1$ mA; $i = 5-10$ mA/cm²) and in 30% KOH saturated with zincates (Figures 31 and 32) showed places penetrated simultaneously by heavy sponge and foam.

2.2 Zinc Penetration in Regular Ag/Zn Cycled Cell

Separators were taken out of a 12 AH Ag/Zn cell which had been charged at 40 mA/in² and discharged at 60 ma/in² for 130 medium cycles. KOH concentration was 42%. Wet life was 6 months. The separator was C19 (silver-treated regenerated cellulose). A number of pictures were taken at 40 ; 100 x and 1000 x at penetrated regions. The penetrated region at 40 x (Figure 33) suggests dendritic penetration. At 1000 x it is visible that the penetrated place consists of a number of fine penetrated spots

(Figure 34). Penetration here can be classified as belonging to the heavy sponge type. The characteristic disappearance of color in the penetrated regions was observed.

The dark yellow color of C19 comes from silver treatment. To determine the mechanism of color removal, separator samples were extracted with a number of complexing agents until the yellow color disappeared. The materials and times were: 1 N NaCN for 30 minutes, 1:1 NH_4OH for 90 hours and 0.1 N $\text{Na}_2\text{S}_2\text{O}_3$ for 90 hours. Also, a sample of C19 was extracted 20 times during 20 days with 27% KOH. The bleached separator from the cycled Ag/Zn cell was examined for silver by polarograph; no Ag was found. It was therefore concluded that all of the silver present is in the argentous state, and that the absence of color around penetrated places means that the argentous silver was extracted. The most likely process appears to be reduction of argentous Ag to metallic Ag by the metallic zinc on its course through the separator.

2.3 Kinetic Study of Zn Deposition

The conditions of deposition of zinc in the micro-cell experiments correspond to the conditions in the Ag/Zn cell existing at the end of charging or at early stage of overcharge. This is that part of cycle during which penetration is most likely to occur. In the micro-cell the zinc anode was placed close to the cathode wrapped in separator. Oxidation of the cathode maintained the concentration of zincate on the anodic side of the separator - constant. Figure 35 shows the change of current with time at constant cathodic potential, of two cells with wrapped and non-wrapped cathodes. The current in both cells decreases initially about three-fold. This is due to concentration polarization resulting from formation of the diffusion layer. After about 10 minutes, the surfaces of both cathodes become covered by dendritic deposit. The surface of the electrodes thus increases. Current through the unwrapped cathode starts rising again. Current through the wrapped cathode instead reaches a plateau and does not change with time. This means that the process is limited there by the diffusion of zincate through the membrane. Consequently, the wrapped cathode is polarized more, and a different type of deposit is obtained.

As the concentration polarization with respect to zincates increases, the chance of hydrogen evolution increases. At overpotentials higher than 30-50 mV slow formation of H_2 bubbles becomes visually evident. It follows that the potentials we are dealing with in this problem are mixed potentials of zinc deposition and hydrogen evolution. Consequently, hydrogen evolution parameters must be known as well as those of Zn deposition. Some of the parameters of H_2 evolution on zinc were determined in 44% KOH (no zincate). The Tafel slope was found to be 110 mV; the exchange current was of the order of 10^{-9} A/cm². The potential of the reversible hydrogen electrode in 44% KOH (with or without zincates) was + 0.48 V versus zinc in saturated zincate in the same KOH concentration.

In accordance with these data, hydrogen evolution becomes significant at overpotentials of 50-100 mV, but it must evolve, even if at extremely low rate, at all potentials at which zinc plates out. Plating on stationary electrodes from solutions of zincates leads always to deposits with high roughness factors. To study the deposition on moving electrodes, the rotating zinc disc electrode was employed. The schematic diagram of the potentiostatic system used in this experiment is given in Figure 3, where: 1) rotated disc electrode, 2) anode in separate compartment, 3) reference electrode (zinc in zincate) 4) milliammeter-recorder, 5) potentiostat, 6) motor driving the rotating disc (1440 rpm). The solution was 4M KOH saturated with zincate and O_2 was removed by passing N_2 through the solution. To make the weight of deposit comparable for low and high currents, the time was regulated so as to pass an equal number of coulombs at each voltage setting. The potential was raised by 5 mV increments and the plating time was such as to pass 0.05 cb/cm² at each potential.

The results are shown in Figure 36 as a Tafel curve, for increase and then decrease of potential on the same electrode. The small value of hysteresis suggests that the plating is smooth in the investigated range. The small rise of current around 55 mV may indicate a small rise in roughness factor which is negligible in comparison that that on stationary electrodes. Also, visual inspection shows that the deposit is smooth. The calculated diffusion limited current for size and speed of the electrode used in 1.6 M zincate is of the order of many amperes. We operated therefore several orders of magnitude below the currents at which concentration polarization could occur. It can be concluded that if there is no concentration polarization - there is no sponge or foam. Or, reversing this conclusion, concentration polarization (and consequently concentration overpotential) must be involved in the formation of each of the above mentioned types of rough plating. The greatest total overvoltage is associated with dendrite formation.

In considering the mechanism of the formation of foam versus dendrites, it became apparent that the area of foam is so large that current density must be very low. At very low current density, corrosion could conceivably take place simultaneously. To study this possibility, galvanostatic transients were run on porous zinc plates, as a first step.

The set up is shown in Figure 4 where: 1) cathode (electroplated zinc or sheet), 2) anode, 3) reference electrode, 4) fast mercury relay, 5) decade resistor box, 6) D.C. power supply (300 V), 7) oscilloscope with Polaroid camera. Typical transients are shown in Figure 37. They were taken on an electroplated zinc electrode in 4M KOH. The electrode was first reduced by cathodic current and then immediately transient 1) was taken. After 2 minutes of wet stand transient 2) was taken. The transition time (τ) of transient 2) was much greater. The transition time is due to reduction of $Zn(OH)_2$ to Zn by the cathodic current. When the total amount of $Zn(OH)_2$ is reduced the potential rises. Transients repeated after longer times than 2 minutes give the same value of τ . It was concluded therefore that a layer of $Zn(OH)_2$ of constant thickness was formed during 2 minutes

or longer periods due to corrosion of zinc. Calculation showed that the thickness of $Zn(OH)_2$ layer was close to one monolayer.

The next step is to determine the extent of the corrosion process inside the foam.

2.4 Study of Membrane Properties Significant for Penetration

It was shown in section 2.1 that zinc in the process of penetrating a separator grows through it rather than punctures it mechanically. The rate of zinc electrodeposition is in general a function of concentration of zincate. If therefore zinc deposits inside of the separator, the concentration of zincates there is one of major factors of the growth. To determine the concentration of zinc within a separator, a sheet of cellophane was soaked 16 hours in 1M KOH saturated with zincate. It was burned afterwards and the residue was extracted with ammonia buffer and the concentration of zinc was determined polarographically. The concentration of zinc in the liquid within the separator was found to be two times lower than in the 0.98 molar zincate external solution. This means that separator absorbs components of the solution selectively, changing their relative concentrations. It is suggested that the low value of hydration water activity in cellophane is responsible for lower solubility of zincate.

One can therefore suggest an explanation as to how the separator works. As long as ZnO is present in the negative compartment, the negative has enough zincate and grows where its concentration is the highest, avoiding the cellophane. When the concentration of zincates decreases at the end of charge (or at overcharge) penetration into the separator starts.

3. SUMMARY AND CONCLUSIONS

Four distinct types of zinc plating were obtained. The concentration polarization seems to play an important role in this diversification. Smooth plating is obtained when no concentration polarization can take place. This is the condition on the rotated zinc disc electrode in saturated zincate solutions in concentrated alkali hydroxide, and at low zinc overpotentials (e.g. 20 mV). The second type is a light sponge or foam. It is produced on stationary electrodes in the same range of overpotentials and concentrations in which smooth plating takes place on rotating electrodes. This suggests that concentration polarization is involved. The same foam can be produced on rotating discs by using dilute zincate solutions, despite the rapid rotation which brings the rate of liquid flow close to the upper limit for laminar flow. The foam formation in this case is again due to the fact that concentration overpotential is high in dilute solutions.

The foam type of deposit is mechanically weak, soft, and low in density. It consists of a loose network of fine elongated whiskers with diameters ranging from 0.2 to 1 micron. From cathodic transients on porous electroplated zinc, it appears that, at the low overpotentials at which foam is formed, an equilibrium exists within the foam between the rate of deposition and the rate of corrosion. Consequently, plating at a rate in excess of corrosion can occur only at the exterior surface of the deposit. Further evidence for deposition at the tips only, comes from the fact that the whisker diameters are so small and relatively uniform.

The corrosion postulated above should lead to the presence of $Zn(OH)_2$ on the interior surfaces. This hydroxide should show up both qualitatively and quantitatively on cathodic galvanostatic transients. Such work has only recently been initiated and will be continued.

The third type of deposit is dendritic. Dendrites are well-shaped, elongated, branched hexagonal crystals 50-200 microns in diameter. They are formed at overpotentials of 100 mV or higher under conditions such that unrestricted growth is feasible.

Where a membrane restricts growth and the overpotential is also at 100 mV or higher, the fourth type of deposit, a heavy sponge, results. This sponge is actually a later stage of dendrite formation. The deposit initially is dendritic. As deposition continues, the presence of the membrane faces growth to proceed laterally, filling in the interstices to form the nodular sponge.

Electrochemical measurements of hydrogen evolution on zinc show that hydrogen evolution must take place at all zinc plating potentials. Nevertheless because of a low exchange current, it becomes significant only at higher plating overpotentials (over 100 mV). This is the same range of overpotentials at which dendrites and heavy sponge form.

Observation of zinc deposition in the presence of separator has shown that zinc grows within the separator and does not puncture it mechanically. Rapid penetration occurs under conditions corresponding to formation of heavy sponge (e.g. at 100 mV overpotential). At even higher overpotentials typical crystalline dendrites grow in the separator in all directions from the penetrated spot. Separator from cycled silver-zinc cells was penetrated by a heavy sponge type of zinc.

The zinc content of electrolyte absorbed by cellophane separators soaked in saturated zincate proved to be of the order of 1/2 that of the zincate. This suggests that the resistance of cellophane to penetration may be associated with the low absorption or "solubility" of zincate in the membrane. This work is in an early stage. The solubility of zincate in other membranes must be known before any conclusions can be drawn.

4. PROGRAM FOR NEXT QUARTER

1. Quantitative correlation of morphological and crystallographic parameters with electrochemical parameters for zinc deposition will be studied. More specifically, the correlation of diameters and length of whiskers and rate of branching, total surface area, and density of deposits will be investigated as a function of exchange current, overpotential components, and current density distribution. These parameters will be studied on stationary electrodes both wrapped and unwrapped and on rotating disc. The above parameters will be studied as a function of: KOH concentration, zincate concentration, concentration of decay products of cellulose and metallic impurity concentrations.
2. Special attention will be given to the conditions at which zinc foam passes into dendritic and spongy forms. Electron microscope studies will be done. $Zn(OH)_2$ content in foam will be tested by galvanostatic transients.
3. Changes in the concentration of solution components in the separator will be tested and correlated with zinc polarization in the cellophane.

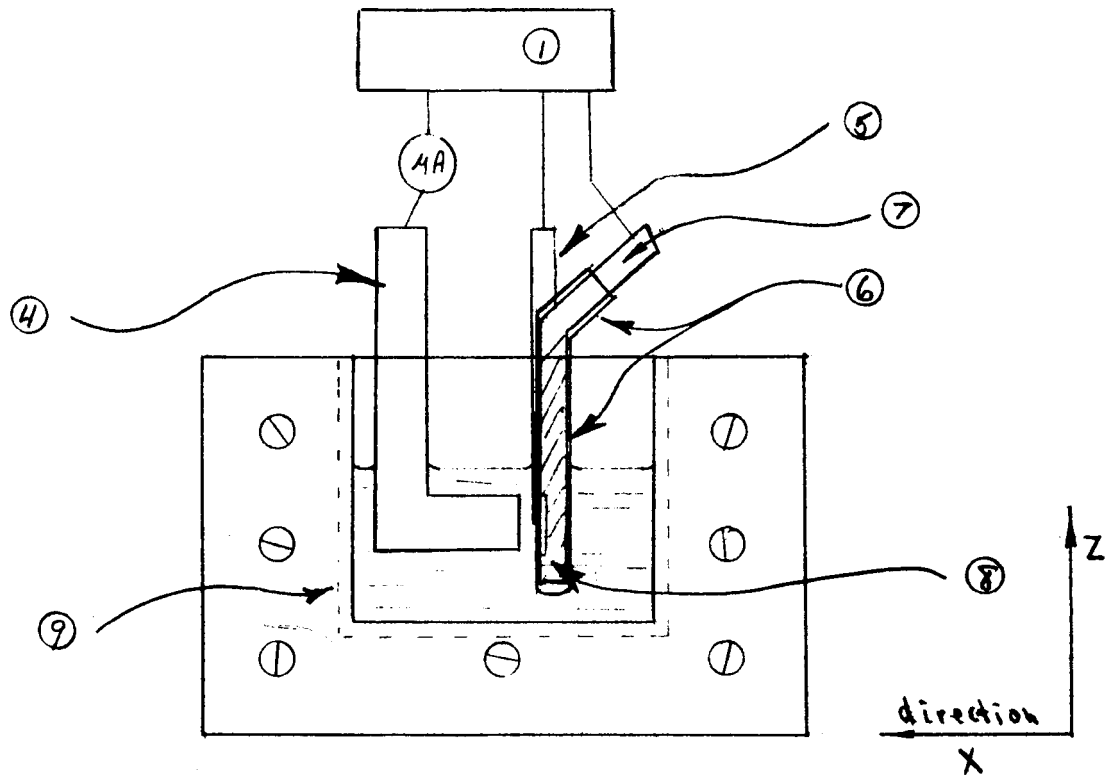


Fig.1 Micro Cell(side)

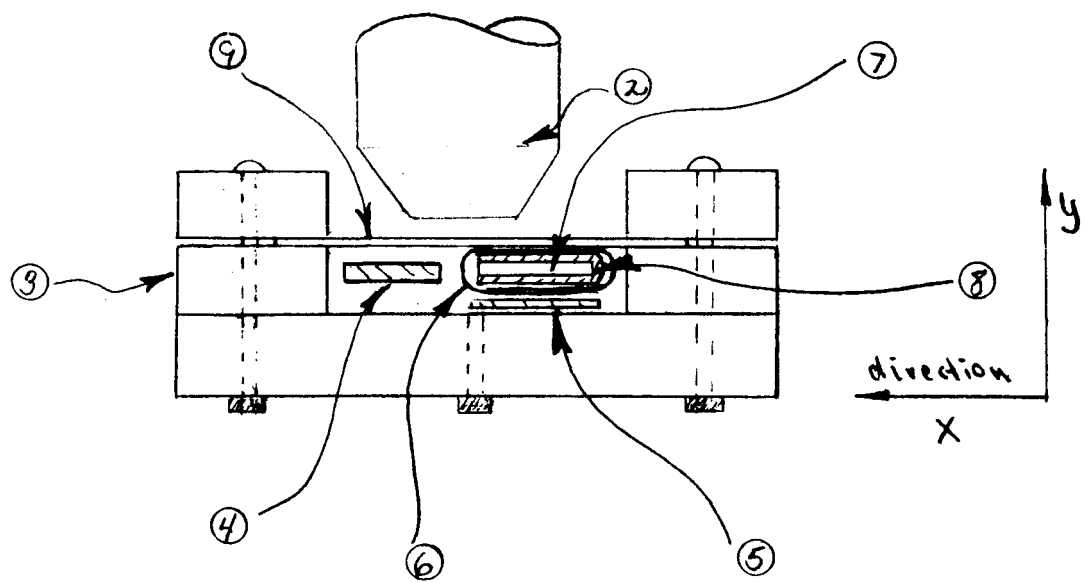


Fig.2 Micro Cell(top)

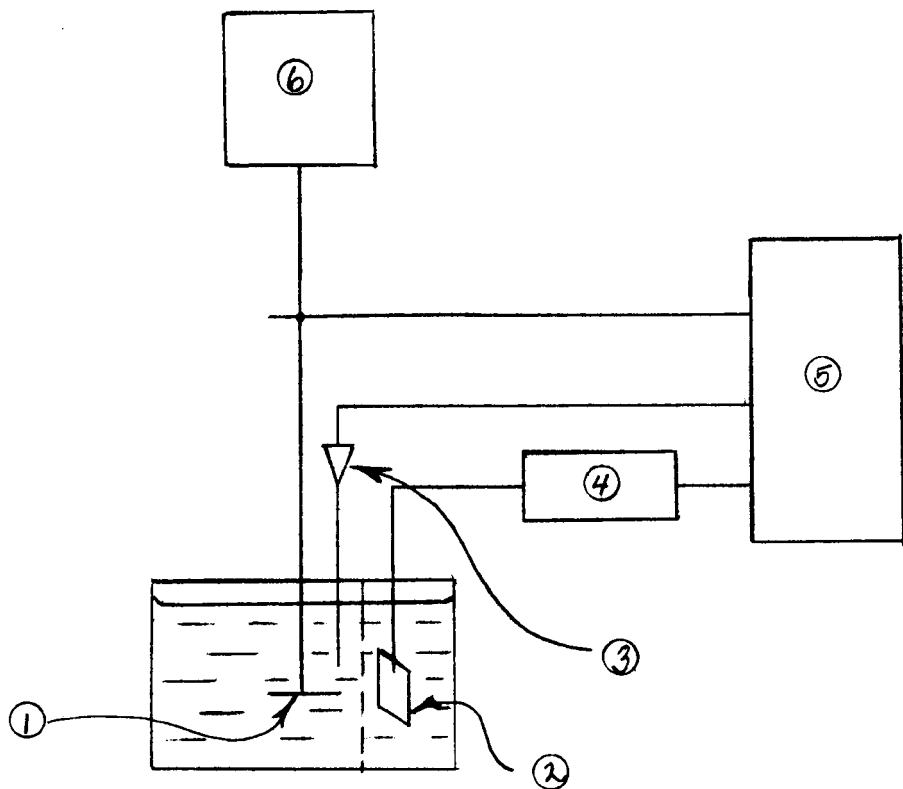


Fig.3 Rotating Disc Apparatus

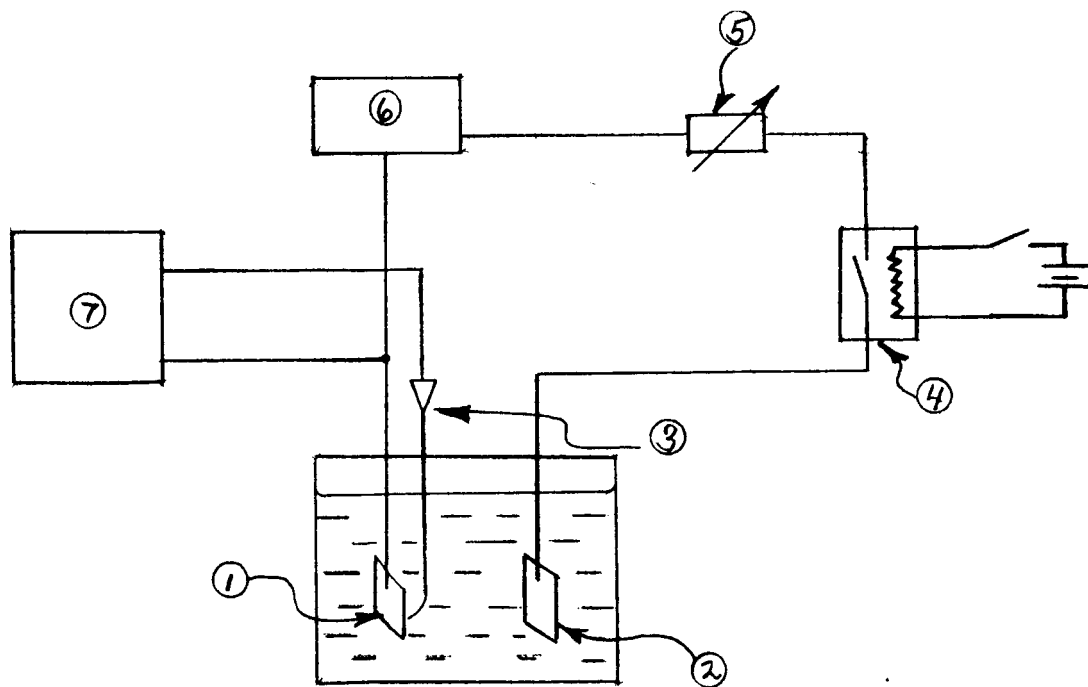


Fig.4 Galvanostatic Transients Apparatus

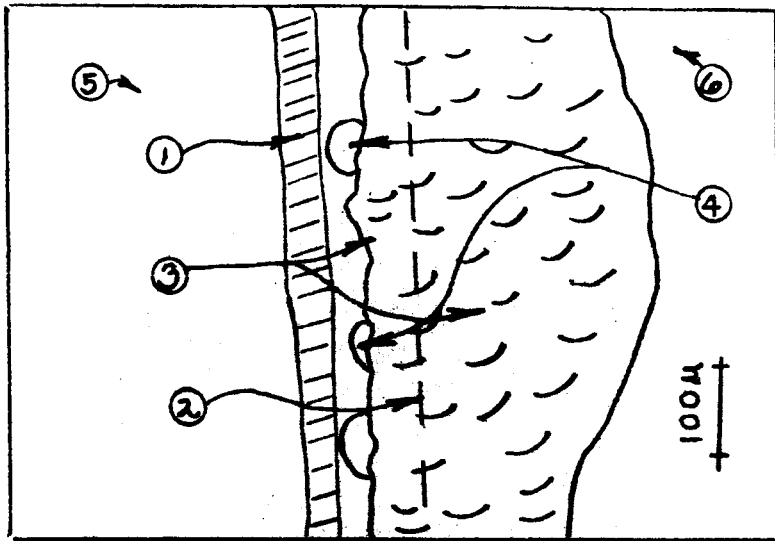


FIG.5'

- 1. Separator
- 2. Initial edge of cathode
- 3. Zinc deposits
- 4. Gas bubbles
- 5. Electrolyte
- 6. Electrode

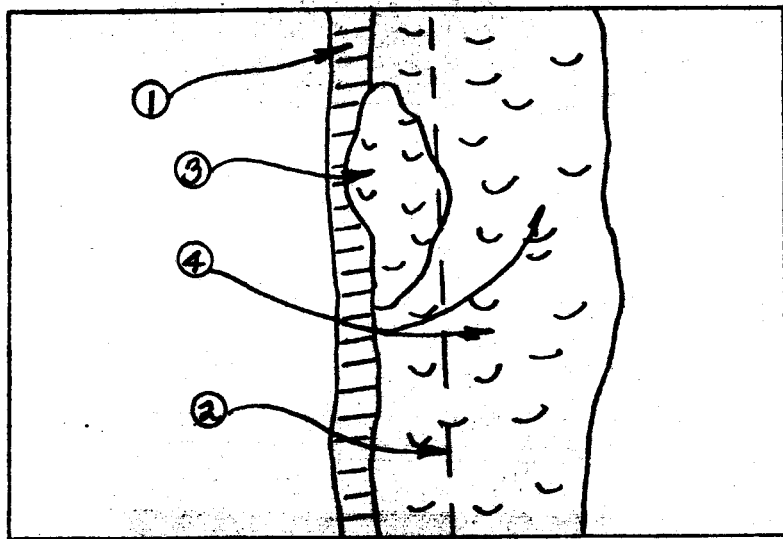


FIG.6'

- 1. Separator (same cell)
- 2. Initial edge of cathode
- 3. Zinc penetration begins
- 4. Zinc deposits

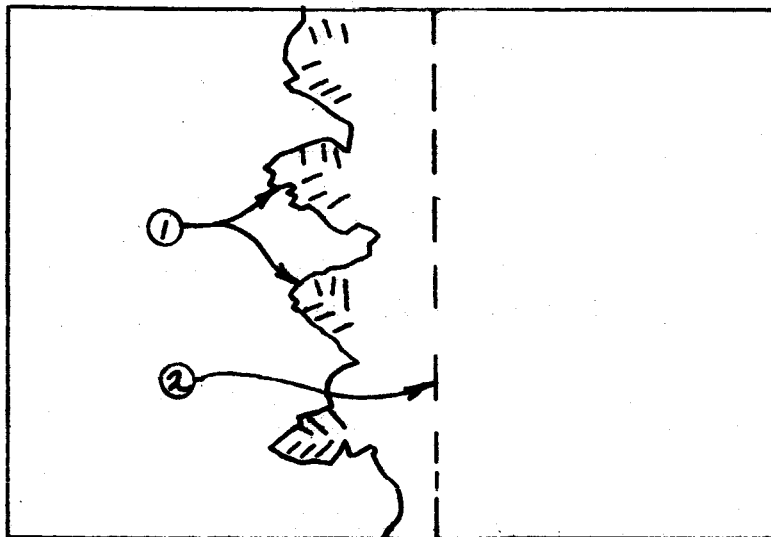


FIG.7'

- 1. Zinc dendrites
- 2. Initial edge of cathode

Figure 5



Potentiostatic deposition of zinc on the cathode wrapped in cellophane, $\eta = 100$ mV
4M KOH saturated with zincate.
Magnification 100 x.
Picture taken after 30 minutes.

Figure 6



Same cathode and experiment.
Picture taken after 21 hours.

Figure 7



Similar conditions as in Fig 5
but the cathode was not
wrapped in cellophane separators.
Picture taken after 30 minutes.

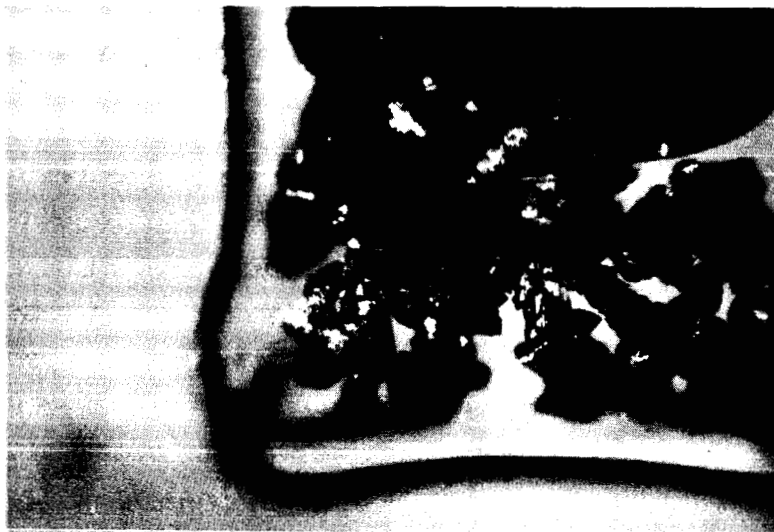


Figure 8

Potentiostatic growth
of Zn dendrites
 $\eta = 100$ mV
4M KOH saturated with
zincates. Picture
taken after 5 hours.
100 x



Figure 9

Same after 21 hours.

Figure 10

Potentiostatic ($\eta = 100$ mV).
Growth of dendrite through
hole in separators. 30% KOH
saturated with zincate after
15 minutes.



Figure 11

Same after 24 minutes.

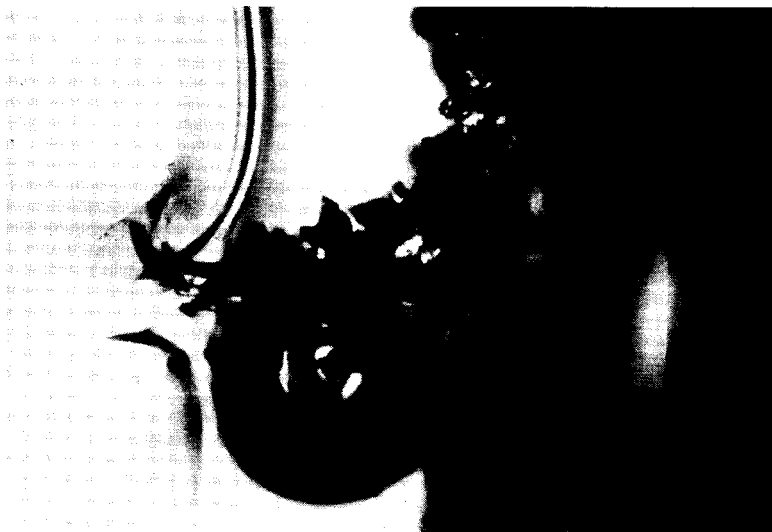
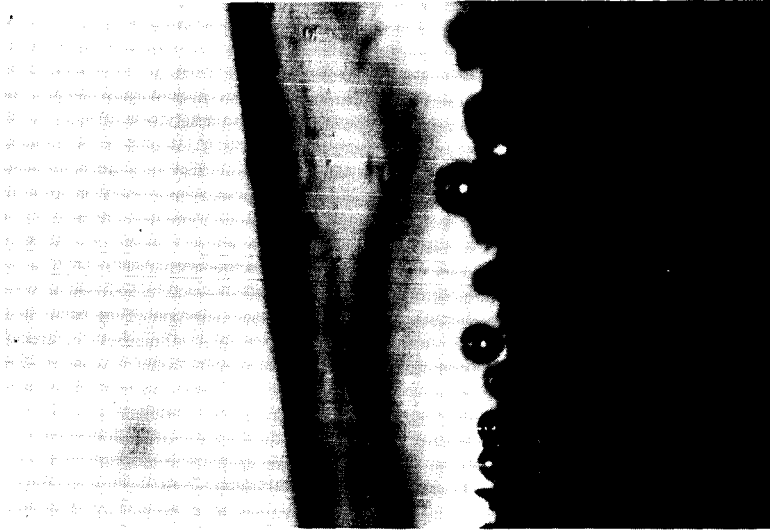


Figure 12

Same after 30 minutes.



Figure 13



Galvanostatic deposition of Zn
in micro cell with a cathode
wrapped in cellophane.
30% KOH saturated with zincate.
 $I = 1 \text{ mA}$ ($i = 5 - 10 \text{ mA/cm}^2$).
Magnification 100 x
Picture taken 10 minutes after
turning current on.

Figure 14



Same experiment.
Picture taken after 55 minutes.

Figure 15

Same after 120 minutes.
100 x



Figure 16

Same after 135 minutes.
100 x



Figure 17

Same after 140 minutes.
100 x





Figure 18

Same after shorting to the
anode. (16 hours)
100 x



Figure 19

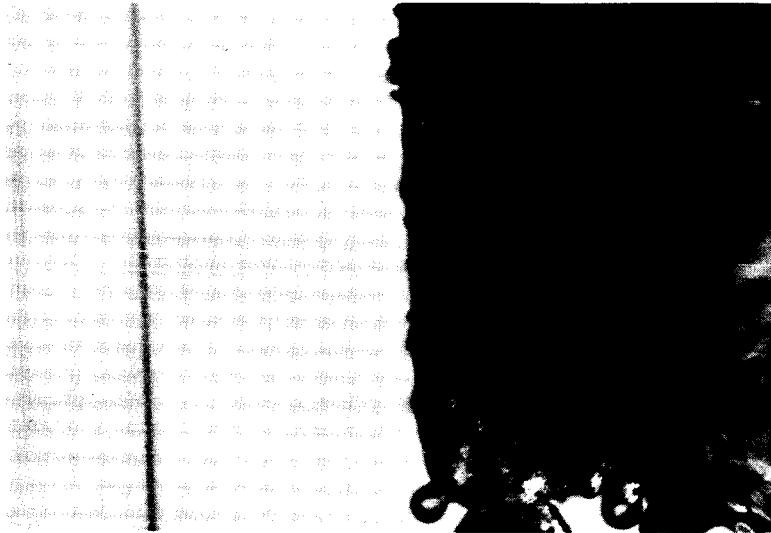
Galvanostatic deposition of Zn.
Identical conditions as
described in Figure 13 but the
cathode was not wrapped.
Picture was taken after
10 minutes.
100 x



Figure 20

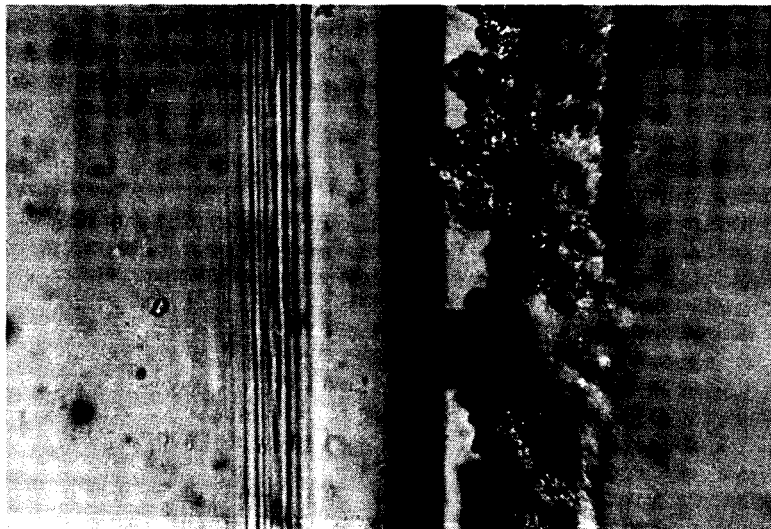
Same cell after 70 minutes,
shortly before it shorted to
the anode.
100 x

Figure 21



Galvanostatic plating at
low rate.
I total = 0.25 mA
44% KOH saturated with zincate
400 x magnification
Beginning of the plating.

Figure 22



Typical foam deposit
after several hours at
above given conditions.
400 x

Figure 23

Typical components of the
foam.

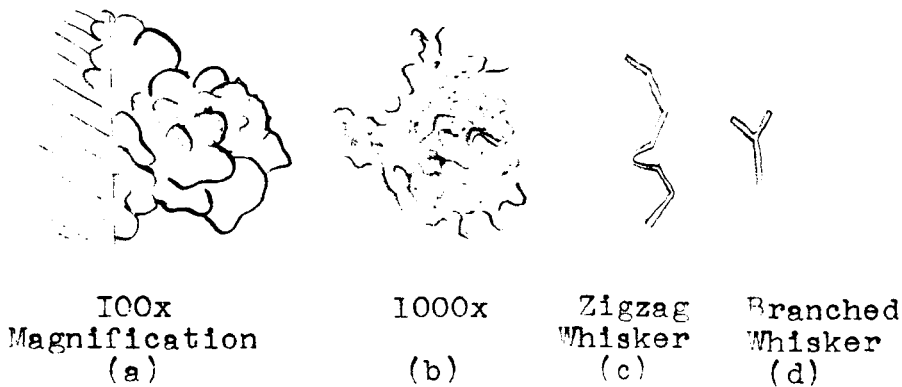


Figure 24



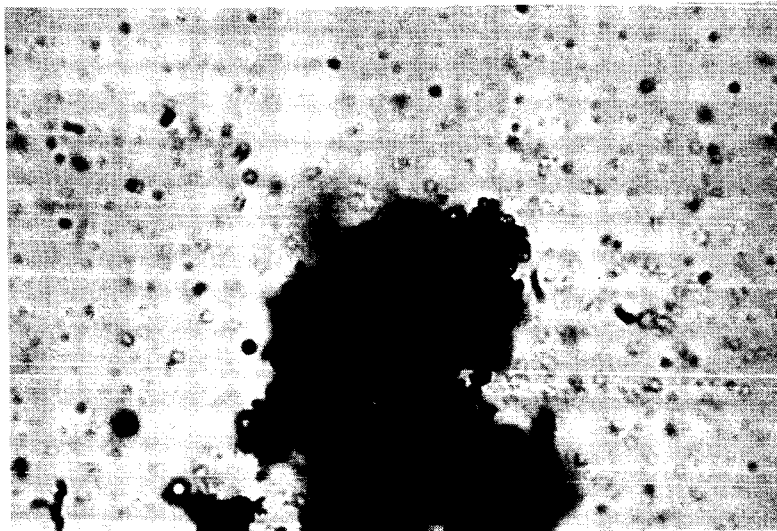
Foam in transmitted light.
Foam formed at low total
current. $I = 0.25$ mA
(2 mA/cm²) with zincate.
400 x

Figure 25



Same foam in reflected light.
400 x

Figure 26

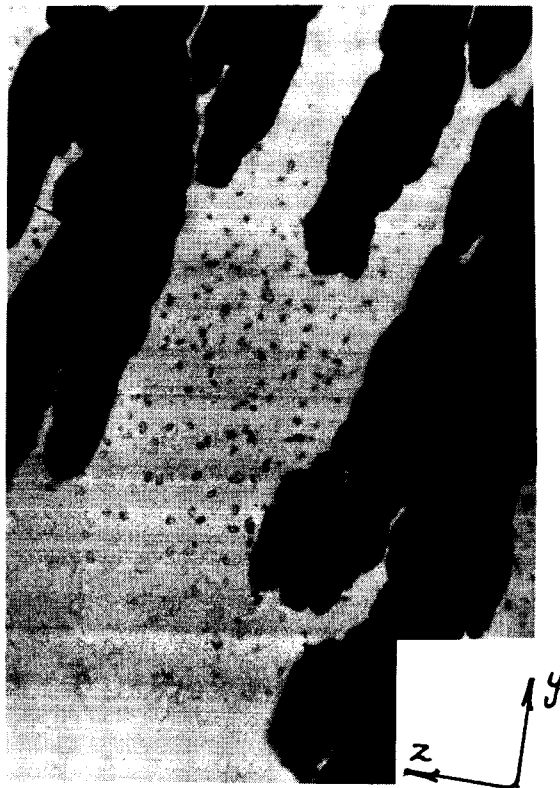


Same foam in immersion oil.
1000 x
Note branched whisker at
lower left corner.

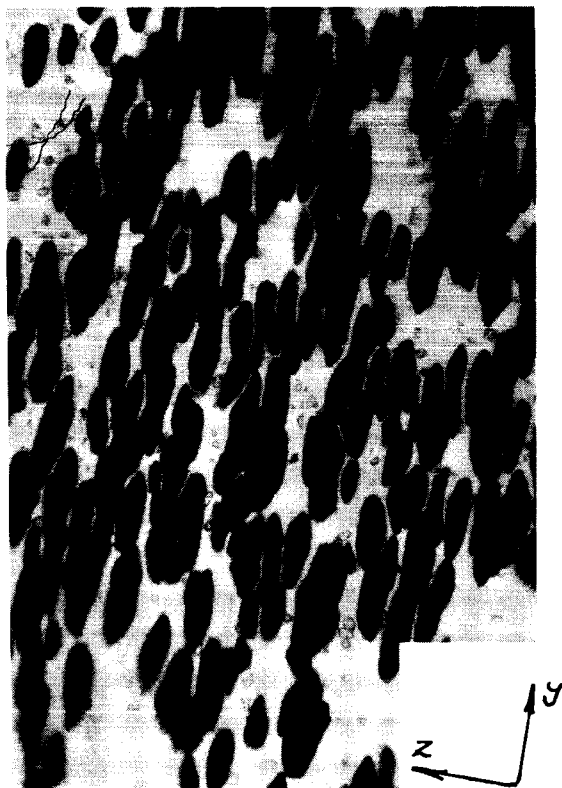
Figure 27 Potentiostatic penetration of Zn through cellophane. $\eta = 200$ mV. Separators penetrated in 1 hour. 44% KOH saturated with zincate.



a. 100 x



b. 400 x



c. 400 x



d. 400 x



Figure 28

Potentiostatic penetration
of Zn into cellophane.

$\eta = 100$ mV

Solution: 44% KOH

Saturated with zincate.

Initial stage of penetra-
tion after 21 hours.

Magnification 100 x



Figure 29

Galvanostatic penetration
of Zn into cellophane.

$i = 15$ mA/cm²

44% KOH saturated with
zincate

40 x



Figure 30

Same separator as in
Figure 29 but magnification
is 100 x.

Figure 31



Separator partially
penetrated by sponge
and foam after
galvanostatic deposi-
tion of Zn in 30% KOH
saturated with zincate.
 $I = 1 \text{ mA}$ ($i = 5-10$
 mA/cm^2). Taken after
16 hour polarization.
100 x

Figure 32



Another spot on the same
separator .
400 x

Figure 33

C-19(300) separator from a
cycled Ag/Zn cell, penetrated
by Zn. Magnification 40 x



Figure 34

Same separator.
Magnification 1000 x



FIG.35

POTENTIOSTATIC DEPOSITION OF Zn

○- cathode wrapped
⊙-cathode unwrapped
 η -100 mV
solution:44% KOH sat. with zincate

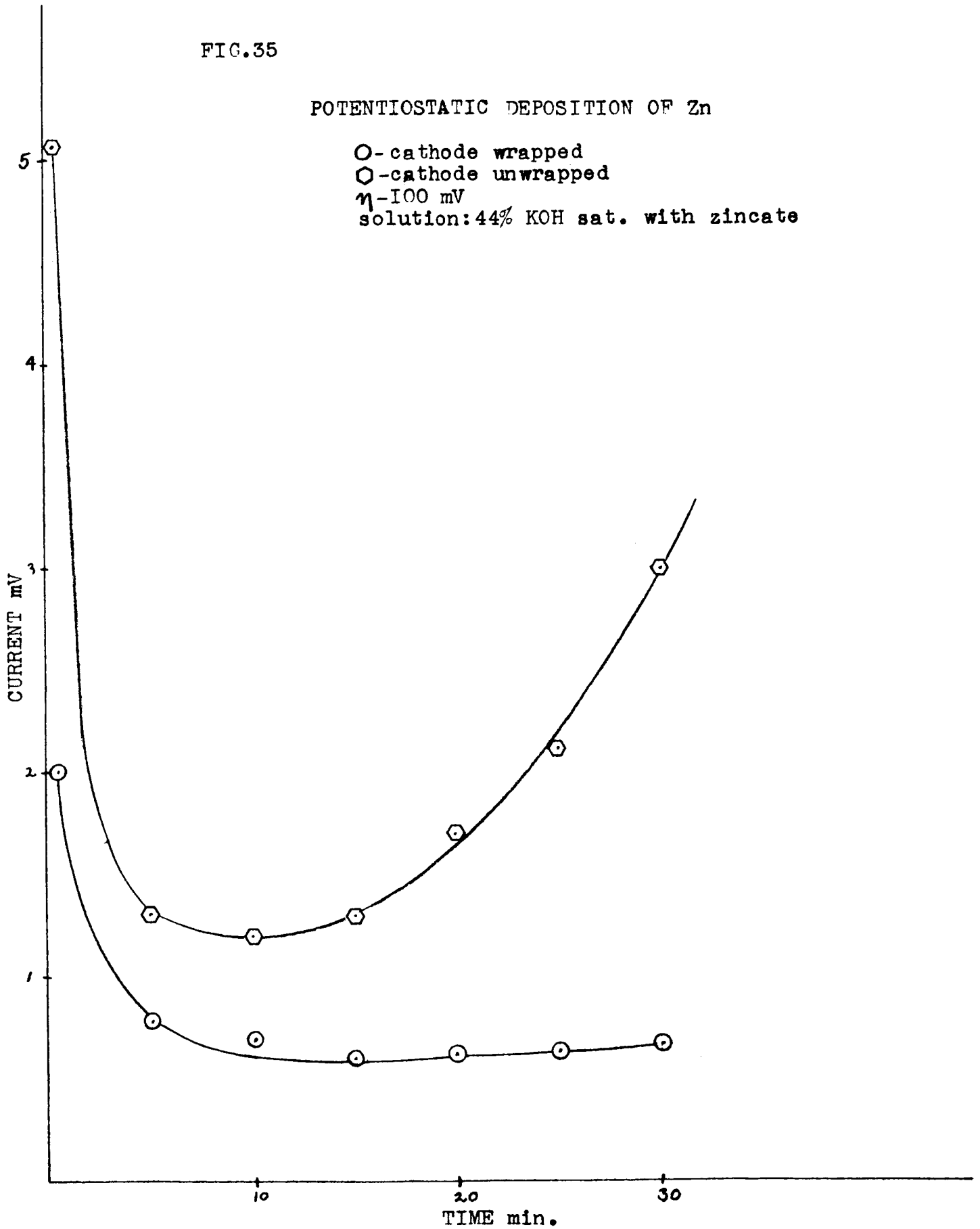


FIG. 36

Potentiostatic Deposition of Zinc on Rotating Disc Electrodes

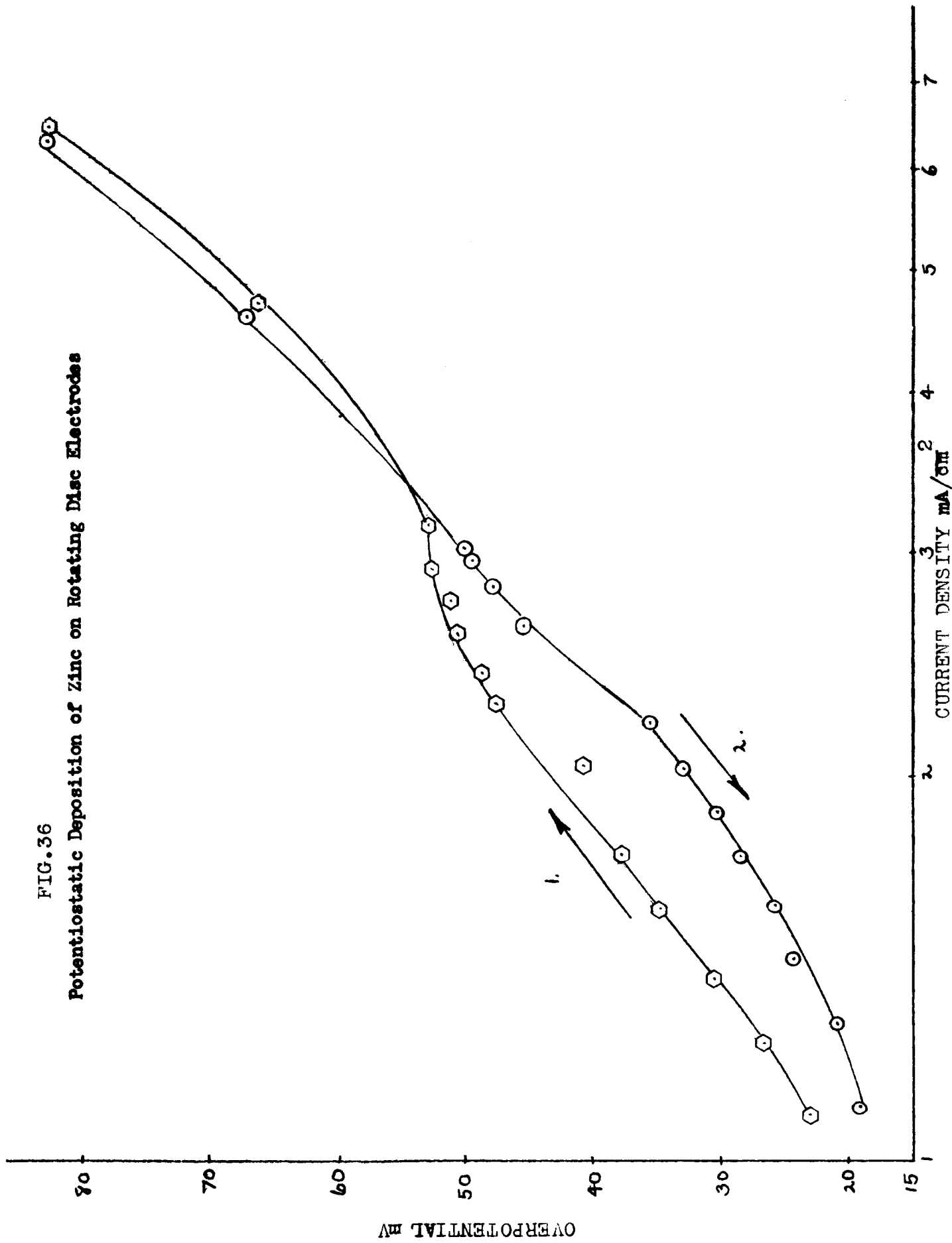


FIG.37 Galvanostatic Transients on Porous Zinc Electrodes

CATHODIC CURRENT $10\text{mA}/\text{cm}^2$

(surface area 2.5cm^2 .)

